Power Dependence of the Shift Caused by Spurious Spectral Components in Atomic Fountain.

F. Levi[12*], J.H. Shirley[2], T.P Heavner[2], Dai-Hyuk Yu[23] and S.R. Jefferts[2]
[1] *INRiM – Str Delle Cacce 91- 10135 Torino Italy*
[2] *NIST-Time and Frequency Division - 325 Broadway Boulder, CO 80305 USA*
[3] *KRISS, 1 Doryong, Yuseong, Daejon 305-340 Korea*
**Electronic address: levi@inrim.it*

In this paper we analyze the behavior of the frequency shift caused by a spurious spectral component in the microwave spectrum against variation of the excitation microwave field. The theory of the shift caused by the presence of spurs in the microwave spectrum was investigated in depth over many years, however for historical reasons the behavior was never analyzed when microwave power is varied far above optimum. The theoretical predictions are significantly different form the thermal beam case.
Furthermore the pulsed operation of a Fountain, with generally a well defined cycle time, set some new constraints on the size of carrier sidebands even when they are symmetric.

I. INTRODUCTION

For the past several decades, primary frequency standards were based on thermal atomic cesium beams. The thermal velocity distribution of these beam standards in general did not allow operation at high microwave power. High microwave power however became widely used in laser cooled devices to leverage the observation of various frequency shifts related to microwave excitation imperfections. In a typical Cs fountain primary frequency standard a sample of cold atoms passes through the Ramsey cavity at a speed of ~3 m/s with a spread in the average velocity due to the thermal distribution of only ~1 cm/s. Experiments where the Rabi frequency of the atoms in the microwave field is varied to many times the optimum (with pulse areas ranging from $\pi/2$, $3\pi/2$, $5\pi/2$, ... $N\pi/2$ with $N \leq 13$), are commonly used to test for a variety of microwave induced anomalies and frequency shifts. Specifically, frequency shifts related to microwave spectrum, microwave leakage and distributed cavity phase are generally investigated by the use of this method [1-5]. This technique may offer leverage in the detection and calibration of the above mentioned shifts. However, as has been demonstrated for both the case of microwave leakage and distributed cavity phase shifts [6, 7], the behavior of the frequency shift at high power can be quite different from that obtained with an extrapolation performed around the optimum power and the presence of functions periodic in the Rabi frequency, tend to dominate the physical behavior of the shift. Therefore these tests must be carried out with a great deal of care and rigorous attention to the theoretical predictions.

II. THEORETICAL RESULTS

The effect of spurious components in the spectrum of the microwave excitation has been analyzed by many authors [8-10]. A complete theory of the shifts caused by single-sideband spurs in Cs beam primary frequency standards can be found in [11] and is the basis for the analysis reported here. From a theoretical point of view the analysis of the shift in frequency standards based on thermal beams or on laser cooled fountains is indistinguishable, with the exception that in fountain frequency standards integration over the velocity distribution is not strictly necessary. Also, the ratio of the Rabi to Ramsey lengths (l/L) is replaced by the ratio of the respective transit times (τ/T_R) for the varying velocity of the atoms during their ballistic flight in a Fountain cycle. The analytical derivation of the shift carried out in [11] is quite complete and obtained with only the approximations that each excitation has constant amplitude and that the spur power is much smaller than optimum power or the carrier power. We recall here for the reader's convenience the main result obtained for mono-velocity atoms in [11]:

$$\delta\omega = \frac{\tau}{T_R}\frac{b_1^2}{b_0}\left(y + z_1\cos(\Delta T_R) + z_2\sin(\Delta T_R)\right) \qquad (1)$$

where $\delta\omega$ is the frequency shift, τ is the interaction time inside the microwave cavity (Rabi time), T_R is the free flight time (Ramsey time), b_1 and b_0 are the Rabi frequencies of the spur and the carrier respectively, Δ is the detuning of the spur frequency from the carrier, and y, z_1 and z_2 are periodic functions of the excitation Rabi frequency and are given by the following formulae:

$$y = \frac{1}{b_0 \tau \sin(b_0 \tau)} \left\{ \frac{b_0}{\Delta} \cos(b_0 \tau) + \frac{1}{1-(\Delta/b_0)^2} \left(\frac{\Delta}{b_0} - \frac{b_0}{\Delta} \cos(b_0 \tau) \cos(\Delta \tau) - \sin(b_0 \tau) \sin(\Delta \tau) \right) \right\}$$

$$z_1 = \frac{\cos(b_0 \tau)}{b_0 \tau \sin(b_0 \tau)} \frac{1}{1-(\Delta/b_0)^2} \left\{ (\cos(b_0 \tau) - 1) \sin(\Delta \tau) + \frac{b_0}{\Delta} (1 - \cos(\Delta \tau)) \sin(b_0 \tau) \right\} \quad (2)$$

$$z_2 = \frac{\cos(b_0 \tau)}{b_0 \tau \sin(b_0 \tau)} \frac{1}{1-(\Delta/b_0)^2} \left\{ (\cos(b_0 \tau) + 1)(1 - \cos(\Delta \tau)) - \frac{b_0}{\Delta} \sin(\Delta \tau) \sin(b_0 \tau) \right\}$$

It is evident from (2) that at those Rabi frequencies where $b_0\tau$ equals $N\pi$ the shift, given by Eq. (1), diverges. This has no particular physical meaning since at those points no microwave excitation occurs (the transition probability is zero). Further, even with the very narrow velocity distribution in a fountain, the Rabi frequency is not exactly the same for all the atoms.

However the shift behavior is dominated by those divergences and also in this case the precise setting of the excitation power is extremely important to minimize the frequency shift.

Even if it is clear from (1) that the shift is proportional to the spur power (when no other parameter varies with the spur amplitude), this statement is essentially of no practical utility, since as we will show, in almost all practical cases the theory predicts a completely different behavior for variation of the excitation power.

In the following sections of the paper, the analysis of the frequency shift induced by spurs will be divided in two parts, first a spur within the Rabi pedestal $\Delta \leq b\tau$ and second a spur outside the Rabi pedestal $\Delta >> b\tau$.

In the following figures and theoretical evaluations and plots a Rabi time of 10 ms and a Ramsey time of .5 s is assumed if not stated differently in the text.

III. SPUR WITHIN THE RABI PEDESTAL

Within the Rabi pedestal the frequency shift associated with a spur of a given amplitude is a fast varying function of the frequency detuning from the carrier (figure 1). If the excitation power is properly set, this function is smooth, and the shift variation is "proportional" to $1/\tau$, while if the Rabi frequency of the carrier is not exactly set, a fast oscillation, whose frequency is equal to $1/T_R$ appears.

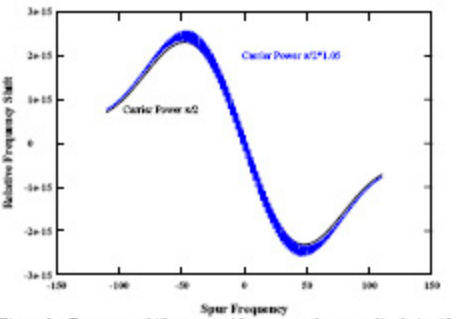

Figure 1 – Frequency shift generated by a spur whose amplitude is -40 dBc, for exact excitation power ($\pi/2$ pulse) and for $1.05 \times \pi/2$ pulse.

At higher excitation power the functional behavior changes completely as can be seen in figure 2. For example, when the excitation power corresponds to exactly a $5\pi/2$ pulse, we find the behavior shown in figure 2. If the spur power is kept constant, the modulus of the shift decreases with respect to the $\pi/2$ case. On the other hand, if the ratio between the spur and carrier power is kept constant, the shift can be either larger or smaller in modulus depending on the spur frequency. A $\pi/2$-$5\pi/2$ test (for example) to enhance the shifting effect of a generic spurious component can therefore be meaningless unless it is carefully coordinated with the appropriate theory.

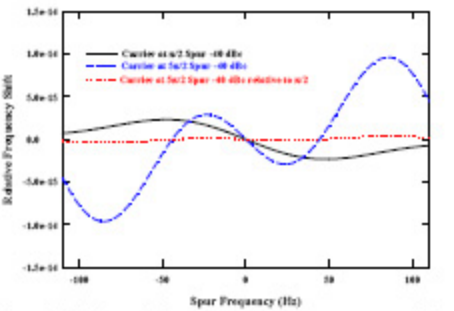

Figure 2 – Shift caused by a spur for excitation power corresponding to $\pi/2$ and $5\pi/2$ pulses

In Fig. 3, we show the prediction and experimental data for the case of a single-sideband spur which is kept at -20 dBc while the frequency of the spur is varied. The data in red triangles are for the case of optimum Rabi frequency so that the pulse area is $\pi/2$

while the data in blue circles are from measurements where the Rabi frequency was such that the pulse area is $3\pi/2$. All of the experimental data shown here were obtained with a Ramsey time of 0.565s and an effective Rabi time of 5.59 ms. The theoretical curves for these conditions, as predicted by Eq. 1, compare reasonably well with the experimental data. We believe the discrepancies between the prediction and data are mostly due to the pulsed operation of the fountain in the case of the $\pi/2$ data while these effects along with small mis-adjustments of the Rabi frequency are probably both apparent in the $3\pi/2$data. The shape of the excitation profile inherent in the theory is different from the experimental excitation profile which is most evident at spur detuning larger than half the Rabi width (~15 Hz).

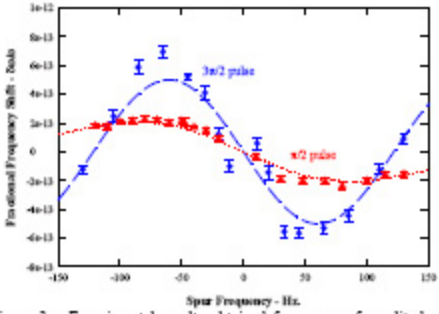

Figure 3 – Experimental results obtained for a spur of amplitude -20dBc for excitation power corresponding to $\pi/2$ and $3\pi/2$ pulses.

We now analyze the frequency shift with excitation power in the neighborhood of optimum excitations, i.e., where the transition probability approaches unity. We find that the value of the frequency shift depends strongly on both how closely optimum microwave power is obtained and on the details of the spur frequency relative to the Rabi and Ramsey times. In Fig. 4, the value of the frequency shift caused by a spur 50 Hz from the carrier as well as one at 49 Hz, with a power -40 dBc is shown for the cases of optimum power, optimum power ±1% and optimum power ±2 % for the lowest occurrences of unity transition probability. It is difficult to set the excitation power at optimum better than a fraction of a percent in practice, both because the atom trajectory through the microwave cavity as well as variations in its velocity affect the optimum microwave power. It is evident from the striking differences between these two curves that the behavior of the frequency shift is quite rich. The value of the frequency shift at high microwave excitation amplitudes is dominated by whether the microwave field is slightly above or below optimum amplitude in the case of a 50 Hz spur while a very small change in the spur frequency causes the frequency shift to be essentially unaffected by small variations in the microwave field amplitude. The measured frequency shift at a given multiple of $\pi/2$ may therefore be determined mostly by the fact that the microwave power is different from optimum power and or by the details of the spur frequency with respect to the Rabi time. Small changes in launch velocity can therefore change the frequency shift associated with a spur in a relatively large fashion. Given the apparent large sensitivity to these effects it seems quite difficult in practice to use high power microwave tests alone to look for frequency shifts caused by spurs in the microwave spectrum.

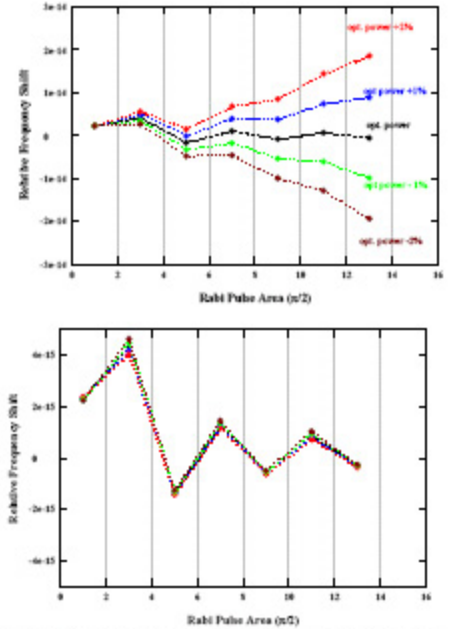

Figure 4 - Frequency shift calculated for a spur at 50 Hz and 49 Hz, for excitation powers not precisely set.

IV. SPUR OUTSIDE THE RABI PEDESTAL

A different behavior can be observed when the spur lays well outside the Rabi pedestal. For spur frequencies up to few hundred Hz, small oscillations are still present, however the behavior of the shift becomes quickly monotonic for spur frequencies well outside the Rabi pedestal; the shift decreases with respect to the spur frequency as $1/\Delta$ (figure 5). In figure 5 the frequency of a spur, whose amplitude is -40dBc, is varied from 200 Hz to 10 kHz.

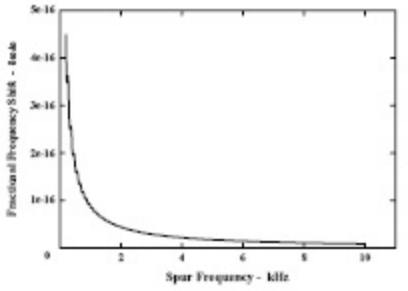

Figure 5 – Frequency shift calculated for a spur outside the Rabi pedestal

Analyzing the behavior of the spur with respect to the excitation power, when the spur frequency is well outside the Rabi envelope, the behavior of the shift changes dramatically because the y term in (1) becomes dominant as the Ramsey structure diminishes. The period of the singularities doubles with respect to the previous case, occurring at $b_0\tau=2N\pi$, and the behavior shown in Fig. 4 changes to a strong oscillation in the frequency shift pattern. "Bi-stable" linear behavior with microwave amplitude (and not power) can be observed, as shown in figure 6.

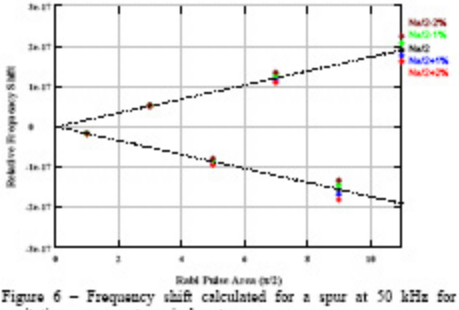

Figure 6 – Frequency shift calculated for a spur at 50 kHz for excitation powers not precisely set.

If the Rabi frequency of the carrier is changed without changing the spur amplitude, (this can be the case of an experiment where the carrier power is changed through the RF channel of a Mixer, while the Spur is originated in the LO channel), the magnitude of the shift decreases with increasing excitation power (figure 7).

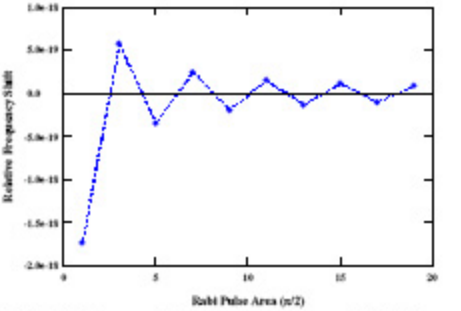

Figure 7 - Frequency shift calculated for a spur at 50 kHz whose amplitude is fixed while the carrier is varied.

V. PULSED OPERATION

Because most fountain frequency standards operate in the pulsed regime, it is worthwhile to examine the consequences of pulsed operation. If we consider the time-domain picture of the microwave field as seen by the atoms it is generically similar to that shown in Fig. 8. The microwave field is zero until the atom enters the Ramsey cavity. It turns on smoothly to a maximum and then turns off smoothly back to zero over a time τ (the Rabi time). The microwave field is then zero for a time T_R (the Ramsey time) at which point the microwave field again turns up smoothly to a maximum and then back to zero. This pattern is then repeated for each cycle of operation.

Suppose an unwanted pure frequency modulation at frequency ω_1 is present on the carrier. The extraneous phase introduced by this modulation can be written as:

$$\beta\cos(\omega_1 t) \qquad (3)$$

where β is the modulation index ($\beta=\Delta f/f_1$ where Δf is the frequency deviation produced by the frequency modulation). We assume that the atoms are centered in the cavity on the way up at t_1 and again on the way down at $t_2=T_R+t_1+\tau$, where $\tau=0$ is taken as the launch time. The change in phase between the two interactions due to the modulation is then given by:

$$\delta\varphi=\beta\left[\cos\omega_1 t_2-\cos\omega_1 t_1\right]= -2\beta\sin\omega_1\left(t_1+\tfrac{1}{2}T_R+\tfrac{1}{2}\tau\right)\sin\omega_1\left(\tfrac{1}{2}T_R+\tfrac{1}{2}\tau\right) \qquad (4)$$

Associated with this phase difference would be a frequency shift of order $\delta\varphi/T_R$. N fountain cycles later

the phase difference would be the same, with t_1 augmented by NT_{cycle}

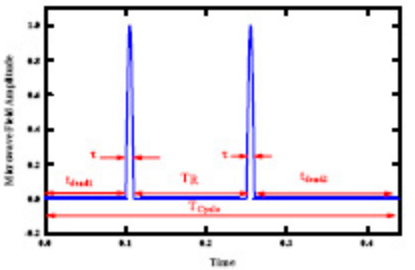

Fig. 8 - Amplitude modulation of the microwave power, as seen by the atoms, during a fountain cycle.

As long as $\omega_1 T_{cycle}$ is not an integer times π (or an integer times a rational fraction of π), this phase difference and any accompanying shift will average to zero after many fountain cycles. But if, for example, the modulation frequency is 50 Hz and the cycle time is exactly 1.020 s (51 cycles at 50 Hz), the same phase difference will occur during each fountain cycle and the associated shift will persist.

From a frequency point of view the microwave spectrum effectively has all the harmonic components that are multiples of $1/T_{cycle}$. If one of these spectral components is coincident with a component of the frequency modulated spectrum, it will produce an asymmetric sideband. Hence balanced sidebands present in the synthesizer can cause frequency shifts, because the pulsed operation of the fountain automatically generates amplitude sidebands that may interfere.

VI. CONCLUSIONS

Given the extremely complex behavior of the frequency shifts caused by the presence of spurious components in the microwave excitation spectrum, we conclude that high-power microwave tests are not well suited for the detection of anomalies due to the presence of spurious component in the microwave spectrum. And these test when applied should be carefully analyzed by comparison with appropriate theory. In general, no leverage can be expected with experiments carried out at higher excitation power. The amplitude and sign of the shift can vary widely, depending on the spur frequency, the Rabi-pedestal width, the Ramsey time and whether the microwave power is slightly above or below optimum. It is therefore very difficult to correct for shifts related to spectral components. This difficulty is compounded by the pulsed operation and possible synchronicity between the spur frequency and the fountain cycle time. Therefore, to guarantee a given level of accuracy in a fountain frequency standard, we must estimate the maximum ratio of acceptable spur to carrier in the spectrum, and ensure that this ratio has been met with independent measurements. For example, assume that a fountain is operated with T_R = 0.5 s and τ = 0.01 s and must be accurate at fractional level of 1×10^{-16} level. A spur within the Rabi pedestal must be reduced to almost -60 dBc. For a spur far off resonance the constraints are more relaxed since larger detuning allow higher spur powers. For example, a spur 50 kHz from the carrier can be -20 dBc and still allow an accuracy of 1×10^{-16}.

REFERENCES

[1] S.R. Jefferts, et al., Metrologia 39 pp. 321-336 (2002).
[2] S. Weyers, U. Hübner, R. Schröder, Chr. Tamm, and A. Bauch, Metrologia 38 pp 343-352. (2001).
[3] F. Levi, L. Lorini, D Calonico, A. Godone, IEEE trans UFFC. 51 10 p 1216 (2004).
[4] K. Szymaniec, W. Chalupczak, P.B. Whibberley, S.N. Lea, D. Henderson, 42 pp. 49-57. (2005) .
[5] C.Vian, et al., IEEE Trans I.M., 54(2) pp.833 (2005)
[6] F. Levi, J.H. Shirley, S.R. Jefferts, to appear on IEEE Trans UFFC.
[7] S.R. Jefferts, J.H. Shirley, N. Ashby, E.A. Burt, G.J.Dick IEEE Trans UFFC 52(12) pp 2314-2321 (2005).
[8] N.F. Ramsey, Phys. Rev 100 4 p 1191 (1955)
[9] J.H. Shirley, J. Appl. Phys. 34 4 (part1) p 783 (1963)
[10] C. Cohen-Tannoudji, Metrologia 13 pp 161-166 (1977).
[11] C. Audoin, M. Jardino, L.S. Cutler, R.F. Lacey, IEEE Trans on Instr. and Meas. IM27 4 p 325 (1978)
[12] W.D. Lee, J.H. Shirley, F.L. Walls, R.E. Drullinger, Proc. 1995 IEEE Intl. Freq. Cont. Symp. pp. 113-118 (1995).